Circular Convolution Filter Bank Multicarrier (FBMC) System with Index Modulation

Jian Zhang*, Minjian Zhao*, Lei Zhang†, Jie Zhong* and Tianhang Yu*
*College of Information Science and Electronic Engineering
Zhejiang University, Hangzhou 310027, China
†5G Innovation Centre (5GIC) and Institute for Communication Systems (ICS)
University of Surrey, Guildford, Surrey, GU2 7XH, UK
Email: lei.zhang@surrey.ac.uk

***Abstract*—Orthogonal frequency division multiplexing with index modulation (OFDM-IM), which uses the subcarrier indices as a source of information, has attracted considerable interest recently. Motivated by the index modulation (IM) concept, we build a circular convolution filter bank multicarrier with index modulation (C-FBMC-IM) system in this paper. The advantages of the C-FBMC-IM system are investigated by comparing the interference power with the conventional C-FBMC system. As some subcarriers carry nothing but zeros, the minimum mean square error (MMSE) equalization bias power will be smaller comparing to the conventional C-FBMC system. As a result, our C-FBMC-IM system outperforms the conventional C-FBMC system. The simulation results demonstrate that both BER and spectral efficiency improvement can be achieved when we apply IM into the C-FBMC system.**

***Index Terms*—FBMC, circular convolution, index modulation, spectral efficiency, BER performance**

I. Introduction

As one of the multicarrier modulation (MCM) systems, orthogonal frequency division multiplexing with index modulation (OFDM-IM), which can be regarded as an extension of the spatial modulation (SM) concept [1] into frequency domain, has attracted considerable interest recently [2]–[4]. At the transmitter of the OFDM-IM system, the subcarriers are divided into groups and the active subcarrier indices are used as a source of information. At the receiver, the subcarrier indices are detected by a maximum likelihood (ML) detector or a low-complexity log-likelihood ratio (LLR) detector [2]. By the utilization of subcarrier indices as a source of information, the OFDM-IM system exhibits an improvement in bit error rate (BER) performance compared to the conventional OFDM system, especially for low-to-mid rate cases [4].

As another MCM system, filter bank multicarrier (FBMC) can provide the best out of band emission [5] among the new waveforms proposed for 5G and future networks, such as generalized frequency division multiplexing (GFDM) [6], universal filtered multi-carrier (UFMC) [7]–[9], filtered orthogonal frequency division multiplexing (F-OFDM) [7] and their variants. This advantage enable the FBMC system to utilize the fragment frequency bandwidth in a spectrum efficient way. Apart from its advantage of significantly reduced out-of-band (OoB) emission, FBMC can achieve higher spectral efficiency as it does not use any cyclic prefix (CP). However, due to the fact that there exists the ramp-up and ramp-down problem at the beginning and end of the frame in FBMC system [10], the spectral efficiency of the FBMC system decreases in the applications with short messages, such as machine-to-machine (M2M) communications and internet of things (IoT) [11], [12].

To improve the spectral efficiency of the conventional FBMC system, the authors in [10], [13] proposed the truncation tails methods. However, the orthogonality of the edge symbols will be degraded due to emitting the signal tails. The orthogonality problem was solved in [14] by replacing the linear convolution operator used in the conventional FBMC system with circular convolution. cyclic prefix (CP) is inserted in front of each block to achieve free interblock interference (IBI). The circular convolution FBMC (C-FBMC) proposed in [14] lighted the passion of the following researchers. Walsh-Hadamard precoding scheme was applied to C-FBMC in [15], which harvests frequency diversity in frequency selective channel. To make C-FBMC perform well in double-dispersive channel, circular fast convolution based FBMC (CFC-FBMC) system was proposed in [16]. Among all of the C-FBMC schemes, the IM technique has not been used in the C-FBMC system before. It has been proved in our previous paper [17] that IM technique can decrease the interference power and provide a better signal to interference ratio (SIR). To enhance the performance of the C-FBMC system in multipath channel, we can apply the IM technique into C-FBMC system.

In this paper, we build a C-FBMC with IM (C-FBMC-IM) system model in matrix form. The spectral efficiency and error performance of the C-FBMC-IM system are investigated. As some subcarriers carry nothing but zeros in the C-FBMC-IM system, the minimum mean square error (MMSE) equalization bias power will be smaller comparing to the conventional C-FBMC systems. As a result, our C-FBMC-IM system outperforms the C-FBMC system. The simulation results demonstrate that 1dB performance gain can be achieved for the proposed C-FBMC-IM system when the spectral efficiency of the C-FBMC-IM system is 6.25% higher than that of the C-FBMC system.

The rest of this paper is organized as follows. Section II presents the model of the proposed C-FBMC-IM system. In section III, we give the advantages of C-FBMC-IM by comparing the interference power. Besides, the ML detector and the LLR detector are upgraded for the C-FBMC-IM system. Simulation results of the C-FBMC-IM system are

This work is supported by the Fundamental Research Funds for the Central Universities and the National Science Foundation of China (NSFC) under Grant 91538103.

presented in Section IV. Finally, Section V concludes the paper.

II. System model

The modulating model of the C-FBMC-IM system is illustrated in Fig.1. As we can see, the C-FBMC-IM is a block-based processing system, each C-FBMC-IM block contains N symbols with M subcarriers in each symbol. The subcarriers bearing constellation symbols are defined as active subcarriers, while the subcarriers left blank are defined as inactive ones. For each symbol, a total of A bits are transmitted. The M subcarriers are divided into G groups, with L subcarriers in each group, i.e., $M = LG$. For each group, the incoming p bits are split into two parts, p_1 bits for the index selector and p_2 bits for the mapper.

On one hand, the first p_1 bits are fed to the index selector and k out of L subcarriers are activated according to the look-up table [2]. Therefore, the number of bits carried by the indices of active subcarriers is given by $p_1 = \lfloor \log_2 C_L^k \rfloor$, where $\lfloor x \rfloor$ denotes the greatest integer smaller than x and C_L^k represents the binomial coefficient. On the other hand, the remaining p_2 bits are mapped to the activated k constellation symbols. The number of bits carried by the constellation symbols is given by $p_2 = k \log_2 W$, where W stands for a W-ary constellation.

After modulation, each group can be written as

$$\mathbf{S}_g = [0, ..., S_{g,0}, 0, ..., 0, ...S_{g,k-1}, ..., 0]^T \in \mathbb{C}^{Q\times 1}. \quad (1)$$

Here, $S_{g,\omega}$ denotes the constellation symbol for $\omega = 1, ..., k$ and $\mathbf{S}_g \in \Lambda$, where Λ is the set of all possible signal vectors. Then, all groups are sent to the C-FBMC symbol creator, which can be implemented either in a consecutive way [2] or in an interleaved way [18]. The generated n-th C-FBMC symbol can be expressed as

$$\mathbf{s}_n = [s_{0,n}, s_{1,n}, ..., s_{M-1,n}]^T \in \mathbb{C}^{M\times 1}, \quad (2)$$

where $s_{m,n} = \bar{s}_{m,n} + j\tilde{s}_{m,n}$, with $\bar{s}_{m,n}$ and $\tilde{s}_{m,n}$ being the real and imaginary parts of $s_{m,n}$, respectively. For active subcarriers, we assume that $\bar{s}_{m,n}$ and $\tilde{s}_{m,n}$ are independent and identically distributed with $\mathrm{E}\{\bar{s}_{m,n}\} = \mathrm{E}\{\tilde{s}_{m,n}\} = 0$ and $\mathrm{E}\{|\bar{s}_{m,n}|^2\} = \mathrm{E}\{|\tilde{s}_{m,n}|^2\} = \sigma_s^2/2$.

The transmitted C-FBMC-IM symbol vector can also be expressed as $\mathbf{s}_n = \bar{\mathbf{s}}_n + j\tilde{\mathbf{s}}_n \in \mathbb{C}^{M\times 1}$. After the processing of the phase shifter matrix and inverse fast fourier transform (IFFT) matrix, the real branch symbol vector can be expressed as

$$\bar{\mathbf{v}}_n = \mathbf{F}^H \mathbf{\Theta}_n \bar{\mathbf{s}}_n \in \mathbb{C}^{M\times 1}. \quad (3)$$

Here, $\mathbf{\Theta}_n$ is the diagonal phase shifter matrix, which can be defined as

$$\mathbf{\Theta}_n = \mathrm{diag}[e^{-j\pi\frac{(0+2n)}{2}}, e^{-j\pi\frac{(1+2n)}{2}}, ..., e^{-j\pi\frac{(M-1+2n)}{2}}] \quad (4)$$

where the m-th diagonal element is $e^{-j\pi\frac{(m+2n)}{2}}$. $\mathbf{F}$ is the normalized M-point fast fourier transform (FFT) matrix, with $\mathbf{F}^H = \mathbf{F}^{-1}$. All the symbols in a C-FBMC-IM block after parallel-to-serial (P/S) conversion can be written as $\bar{\mathbf{v}} = [\bar{\mathbf{v}}; \bar{\mathbf{v}}_1; ..., \bar{\mathbf{v}}_{N-1}] \in \mathbb{C}^{MN\times 1}$.

For C-FBMC-IM system, the transmitted signal is circular convolved with the filter $\mathbf{g} = [g_0, g_1, ..., g_{KM-1}]$. The real branch filter can be expressed

$$\bar{\mathbf{g}} = [\bar{\mathbf{g}}_0, \bar{\mathbf{g}}_1, ..., \bar{\mathbf{g}}_{K-1}] = [g_0, g_1, ..., g_{KM-1}], \quad (5)$$

where K denotes the overlapping factor. We can define the real branch circular convolution matrix as

$$\bar{\mathbf{Q}} = \begin{pmatrix} \bar{\mathbf{G}}_0 & \bar{\mathbf{G}}_{K-1} & \dots & \bar{\mathbf{G}}_1 \\ \bar{\mathbf{G}}_1 & \bar{\mathbf{G}}_0 & \dots & \bar{\mathbf{G}}_2 \\ \vdots & \vdots & \ddots & \vdots \\ \bar{\mathbf{G}}_{K-1} & \bar{\mathbf{G}}_{K-2} & \dots & \bar{\mathbf{G}}_0 \end{pmatrix} \in \mathbb{R}^{KM\times KM}, \quad (6)$$

where the sub-matrix $\bar{\mathbf{G}}_k$ is given by

$$\bar{\mathbf{G}}_k = \mathrm{diag}[\bar{\mathbf{g}}_k] = \mathrm{diag}[g_{kM}, g_{kM+1}, ..., g_{kM+M-1}]. \quad (7)$$

After being circularly convolved with the filter, the real branch of the transmitted symbol is expressed as $\bar{\mathbf{x}} = \bar{\mathbf{Q}}\bar{\mathbf{v}} \in \mathbb{C}^{MN\times 1}$ with the assumption of $N = K$.

Similarly, the imaginary branch of the transmitted C-FBMC-IM symbol is given by $\tilde{\mathbf{x}} = \tilde{\mathbf{Q}}\tilde{\mathbf{v}} \in \mathbb{C}^{MN\times 1}$, where $\tilde{\mathbf{v}} = [\tilde{\mathbf{v}}_0; \tilde{\mathbf{v}}_1; ..., \tilde{\mathbf{v}}_{N-1}] \in \mathbb{C}^{MN\times 1}$ with $\tilde{\mathbf{v}}_n = \mathbf{F}^H j\mathbf{\Theta}_n \tilde{\mathbf{s}}_n$. Besides, the imaginary branch circular convolution matrix $\tilde{\mathbf{Q}}$ is defined as the same way with the $\bar{\mathbf{Q}}$ by replacing $\bar{\mathbf{G}}_k$ with $\tilde{\mathbf{G}}_k$, where $\tilde{\mathbf{G}}_k = \mathrm{diag}[\tilde{\mathbf{g}}_k]$ with

$$\tilde{\mathbf{g}}_k = [g_{mod(M/2+kM,KM)}, g_{mod(M/2+kM+1,KM)}, ..., g_{mod(M/2+kM+M-1,KM)}]. \quad (8)$$

After adding the real and imaginary branch signals (i.e. $\mathbf{x} = \bar{\mathbf{x}} + \tilde{\mathbf{x}}$), a CP is inserted to cancel the IBI caused by the multipath channel. Suppose the channel is expressed as $\mathbf{h} = [h_0, h_1, ..., h_{L_h-1}]^T$ with the maximum delay L_h. To achieve a IBI free system, the length of CP can not be shorter than L_h. For C-FBMC-IM system. the spectral efficiency can be calculated by

$$\eta_{\mathrm{C-FBMC-IM}} = \frac{N\frac{M}{L}(\lfloor \log_2 C_L^k \rfloor + k\log_2 W)}{NM + L_h}. \quad (9)$$

The C-FMBC-IM system reduces to C-FMBC system in the case of $k = L$, whose spectral efficiency is given by

$$\eta_{\mathrm{C-FBMC}} = \frac{NM\log_2 W}{NM + L_h}. \quad (10)$$

The spectral efficiency gain of the C-FBMC-IM system over C-FBMC system can be expressed as

$$\rho = \frac{\lfloor \log_2 C_L^k \rfloor}{L\log_2 W} + \frac{k}{L}. \quad (11)$$

By properly choosing L and k, the spectral efficiency of the C-FBMC-IM system can be improved. For example, when $(L, k) = (8, 7)$ and $W = 4$, we can calculate $\rho = 1.0625$, which indicates that the spectral efficiency of the C-FBMC-IM system exceeds that of the C-FBMC system.

III. The derivation of the received signal

The receiver process of the C-FBMC-IM system is shown in Fig.2. At the receiver, the received signal block after removing CP is given by

$$\mathbf{y} = \mathbf{h}_c\mathbf{x} + \mathbf{n}, \quad (12)$$

where $\mathbf{n}$ denotes the Gaussian noise with variance σ_n^2 and $\mathbf{h}_c$ is a $NM \times NM$ circulant channel matrix with $\mathbf{h}$ appended

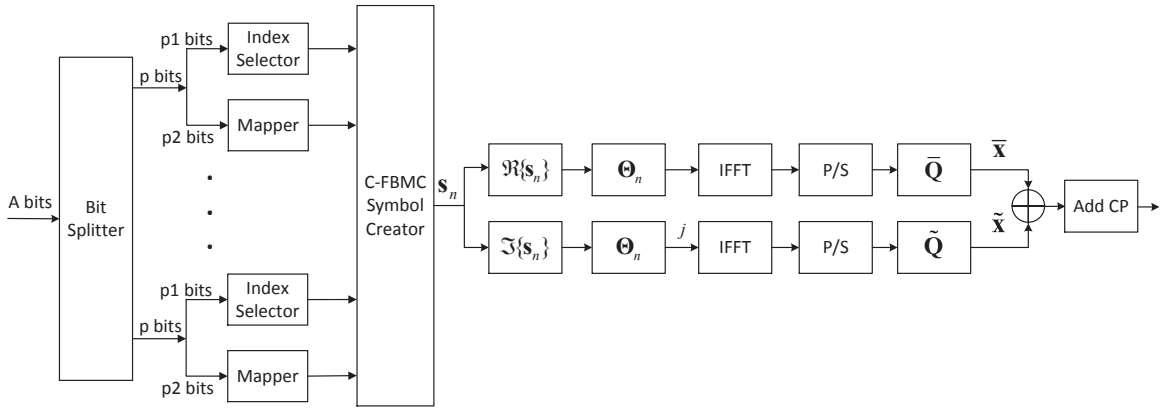

Fig. 1. Block diagram of the C-FBMC-IM transmitter

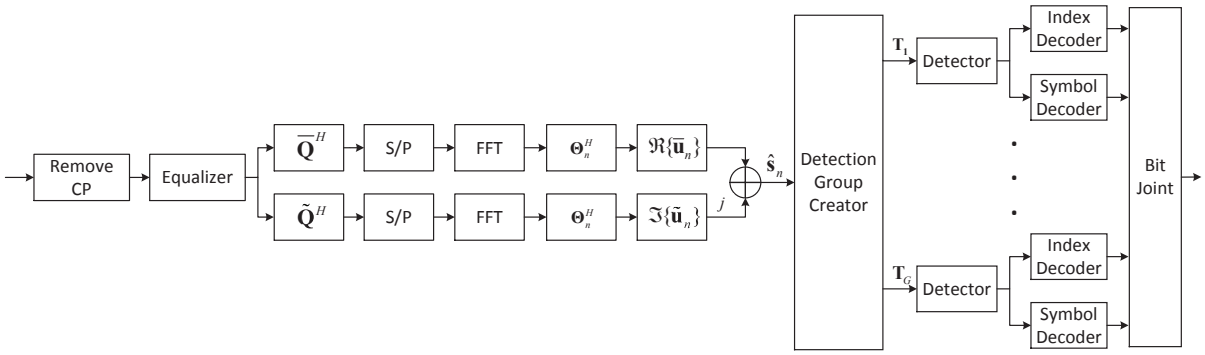

Fig. 2. Receiver process of the C-FBMC-IM system

with $NM - L_h$ zeros in its first column. Furthermore, $\mathbf{h}_c$ can be diagonalized by FFT matrix and it can be expressed as $\mathbf{h}_c = \mathbf{F}_{NM}^H \mathbf{\Lambda} \mathbf{F}_{NM}$, where $\mathbf{F}_{NM}$ denotes the NM-point FFT matrix and $\mathbf{\Lambda} = \text{diag}[H_0, H_1, ..., H_{NM}]$ with H_i being the i-th element of $\mathbf{F}_{NM}\mathbf{h}$.

Transforming the received signal into frequency domain, we can obtain

$$\mathbf{Y} = \mathbf{F}_{NM}\mathbf{y} = \mathbf{\Lambda}\mathbf{X} + \mathbf{N}, \tag{13}$$

where $\mathbf{Y}$, $\mathbf{X}$ and $\mathbf{N}$ are the frequency response of $\mathbf{y}$, $\mathbf{x}$ and $\mathbf{n}$, respectively. Then, the equalization is processed in frequency domain and the channel equalizer diagonal matrix can be expressed as

$$\mathbf{W} = \mathbf{\Lambda}^H(\mathbf{\Lambda}\mathbf{\Lambda}^H + \alpha\sigma_n^2\mathbf{I})^{-1}. \tag{14}$$

Here, $\alpha = 0$ stands for the ZF equalizer and $\alpha = 1$ represents the MMSE equalizer. After equalization, the equalized signal is given by

$$\mathbf{U} = \mathbf{X} + \mathbf{\Gamma}\mathbf{X} + \mathbf{W}\mathbf{N}, \tag{15}$$

where $\mathbf{\Gamma}$ is a MMSE equalization bias diagonal matrix with the i-th diagonal element $(1 - \frac{H_i^2}{H_i^2 + \alpha\sigma_n^2})$. Transforming the equalized signal back to time domain, we can obtain

$$\mathbf{u} = \mathbf{x} + \mathbf{F}_{NM}^H \mathbf{\Gamma} \mathbf{F}_{NM}\mathbf{x} + \mathbf{F}_{NM}^H \mathbf{W} \mathbf{F}_{NM}\mathbf{n}. \tag{16}$$

Then, the same operation will be implemented in the real and imaginary branches independently. In the next, we will take the real branch for example to illustrate the detailed derivation. Firstly, being circularly convolved with the filter, the received signal has the following expression $\bar{\mathbf{p}} = \bar{\mathbf{Q}}^H\mathbf{u}$. For the n-th symbol, $\bar{\mathbf{p}}_n = [\bar{p}_{nM}, \bar{p}_{nM+1}, ..., \bar{p}_{nM+M-1}]^T$. The n-th symbol after FFT processing and phase shifting is expressed as

$$\bar{\mathbf{r}}_n = \mathbf{\Theta}_n^H \mathbf{F} \bar{\mathbf{p}}_n. \tag{17}$$

Using the definition of $\bar{\mathbf{p}}_n$ and substituting (16) into (17), we have the following expression

$$\bar{\mathbf{r}}_n = \sum_{i=0}^{N-1} \bar{\mathbf{V}}_{n,i}\bar{\mathbf{s}}_i + \sum_{i=0}^{N-1} \bar{\tilde{\mathbf{V}}}_{n,i}\tilde{\mathbf{s}}_i + \bar{\mathbf{Z}}_n\mathbf{x} + \bar{\mathbf{B}}_n\mathbf{n}, \tag{18}$$

where $\bar{\mathbf{V}}_{n,i} = \mathbf{\Theta}_n^H \mathbf{F} \bar{\mathbf{Q}}_n^H \bar{\mathbf{Q}}_i \mathbf{F}^H \mathbf{\Theta}_i$, $\bar{\tilde{\mathbf{V}}}_{n,i} = j\mathbf{\Theta}_n^H \mathbf{F} \bar{\mathbf{Q}}_n^H \tilde{\mathbf{Q}}_i \mathbf{F}^H \mathbf{\Theta}_i$, $\bar{\mathbf{Z}}_n = \mathbf{\Theta}_n^H \mathbf{F} \bar{\mathbf{Q}}_n^H \mathbf{F}_{NM}^H \mathbf{\Gamma} \mathbf{F}_{NM}$ and $\bar{\mathbf{B}}_n = \mathbf{\Theta}_n^H \mathbf{F} \bar{\mathbf{Q}}_n^H \mathbf{F}_{NM}^H \mathbf{W} \mathbf{F}_{NM}$ with $\bar{\mathbf{Q}}_n^H$ and $\bar{\mathbf{Q}}_i$ being the n-th and i-th row of the matrix $\bar{\mathbf{Q}}^H$ and $\bar{\mathbf{Q}}$, respectively. For $\bar{\mathbf{r}}_n$, the first term contains the desired symbol (i.e. $\bar{\mathbf{s}}_n$), the second term is an imaginary-valued term, the third term is the MMSE equalization bias term and the last term is the processed noise term.

$\bar{\mathbf{V}}_{n,i}$ have the following properties [19]

$$\bar{\mathbf{V}}_{n,i} = \begin{cases} \mathbf{I} + j\Im\{\bar{\mathbf{V}}_{n,n}\} & (i = n) \\ j\Im\{\bar{\mathbf{V}}_{n,i}\} & (i \neq n) \end{cases}. \tag{19}$$

Taking the real part of $\bar{\mathbf{r}}_n$, the estimated real branch of the

n-th symbol can be expressed as

$$\hat{\bar{\mathbf{s}}}_n = \bar{\mathbf{s}}_n + \Re\{\bar{\mathbf{Z}}_n\mathbf{x} + \bar{\mathbf{B}}_n\mathbf{n}\}. \tag{20}$$

With the same derivation, the estimated imaginary branch of the n-th symbol is given by

$$\hat{\tilde{\mathbf{s}}}_n = \tilde{\mathbf{s}}_n + \Im\{\tilde{\mathbf{Z}}_n\mathbf{x} + \tilde{\mathbf{B}}_n\mathbf{n}\} \tag{21}$$

with the definition $\tilde{\mathbf{Z}}_n = \mathbf{\Theta}_n^H\mathbf{F}\tilde{\mathbf{Q}}_n^H\mathbf{F}_{NM}^H\mathbf{\Gamma}\mathbf{F}_{NM}$, and $\tilde{\mathbf{B}}_n = \mathbf{\Theta}_n^H\mathbf{F}\tilde{\mathbf{Q}}_n^H\mathbf{F}_{NM}^H\mathbf{W}\mathbf{F}_{NM}$.

Finally, combining the estimated real and imaginary branch, the estimation of the n-th symbol can be expressed as

$$\begin{aligned}\hat{\mathbf{s}}_n = \bar{\mathbf{s}}_n + j\tilde{\mathbf{s}}_n + \underbrace{\Re\{\bar{\mathbf{Z}}_n\mathbf{x}\} + j\Im\{\tilde{\mathbf{Z}}_n\mathbf{x}\}}_{\mathbf{I}_{e,n}} \\ + \underbrace{\Re\{\bar{\mathbf{B}}_n\mathbf{n}\} + j\tilde{\mathbf{B}}_n\mathbf{n}\}}_{\mathbf{I}_{\eta,n}}\end{aligned} \tag{22}$$

According to (22), we can see that the desired symbol is affected by the MMSE equalization bias $\mathbf{I}_{e,n}$ and the processed noise $\mathbf{I}_{\eta,n}$, which are independent with each other.

The MMSE equalization bias power can be written as

$$\begin{aligned}\mathrm{E}\|\mathbf{I}_{e,n}\|^2 &= \mathrm{E}\|\Re\{\bar{\mathbf{Z}}_n\mathbf{x}\} + j\Im\{\tilde{\mathbf{Z}}_n\mathbf{x}\}\|^2 \\ &= \frac{1}{2}\Re\{\mathrm{E}\|\bar{\mathbf{Z}}_n\mathbf{x} + j\tilde{\mathbf{Z}}_n\mathbf{x}\|^2\} \\ &= \frac{1}{2}\Re\{\bar{\mathbf{Z}}_n\boldsymbol{\psi}\bar{\mathbf{Z}}_n^H - j\bar{\mathbf{Z}}_n\boldsymbol{\psi}\tilde{\mathbf{Z}}_n^H \\ &\quad + j\tilde{\mathbf{Z}}_n\boldsymbol{\psi}\bar{\mathbf{Z}}_n^H + \tilde{\mathbf{Z}}_n\boldsymbol{\psi}\tilde{\mathbf{Z}}_n^H\},\end{aligned} \tag{23}$$

where $\boldsymbol{\psi} = \mathrm{E}[\mathbf{x}\mathbf{x}^H]$. By using $\mathbf{x} = \bar{\mathbf{Q}}\bar{\mathbf{v}} + \tilde{\mathbf{Q}}\tilde{\mathbf{v}}$, we have

$$\boldsymbol{\psi} = \bar{\mathbf{Q}}\mathrm{E}[\bar{\mathbf{v}}\bar{\mathbf{v}}^H]\bar{\mathbf{Q}}^H + \tilde{\mathbf{Q}}\mathrm{E}[\tilde{\mathbf{v}}\tilde{\mathbf{v}}^H]\tilde{\mathbf{Q}}^H. \tag{24}$$

It is easy to prove that $\mathrm{E}[\bar{\mathbf{v}}\bar{\mathbf{v}}^H] = \mathrm{E}[\tilde{\mathbf{v}}\tilde{\mathbf{v}}^H] = \frac{k\sigma_s^2}{2L}\mathbf{I}$, then the MMSE equalization bias power can be written as

$$\begin{aligned}\mathrm{E}\|\mathbf{I}_{e,n}\|^2 = \frac{k\sigma_s^2}{4L}\Re\{\bar{\mathbf{Z}}_n\mathbf{Q}_c\bar{\mathbf{Z}}_n^H - j\bar{\mathbf{Z}}_n\mathbf{Q}_c\tilde{\mathbf{Z}}_n^H \\ + j\tilde{\mathbf{Z}}_n\mathbf{Q}_c\bar{\mathbf{Z}}_n^H + \tilde{\mathbf{Z}}_n\mathbf{Q}_c\tilde{\mathbf{Z}}_n^H\},\end{aligned} \tag{25}$$

where $\mathbf{Q}_c = \bar{\mathbf{Q}}\bar{\mathbf{Q}}^H + \tilde{\mathbf{Q}}\tilde{\mathbf{Q}}^H$. The processed noise power can be written as

$$\begin{aligned}\mathrm{E}\|\mathbf{I}_{\eta,n}\|^2 = \frac{1}{2}\Re\{\mathrm{E}[\bar{\mathbf{B}}_n\mathbf{n}\mathbf{n}^H\bar{\mathbf{B}}_n^H - j\bar{\mathbf{B}}_n\mathbf{n}\mathbf{n}^H\tilde{\mathbf{B}}_n^H \\ + j\tilde{\mathbf{B}}_n\mathbf{n}\mathbf{n}^H\bar{\mathbf{B}}_n^H + \tilde{\mathbf{B}}_n\mathbf{n}\mathbf{n}^H\tilde{\mathbf{B}}_n^H]\}.\end{aligned} \tag{26}$$

Since $\mathrm{E}[\mathbf{n}\mathbf{n}^H] = \sigma_n^2\mathbf{I}$, we have

$$\begin{aligned}\mathrm{E}\|\mathbf{I}_{\eta,n}\|^2 = \frac{\sigma_n^2}{2}\Re\{[\bar{\mathbf{B}}_n\bar{\mathbf{B}}_n^H - j\bar{\mathbf{B}}_n\tilde{\mathbf{B}}_n^H \\ + j\tilde{\mathbf{B}}_n\bar{\mathbf{B}}_n^H + \tilde{\mathbf{B}}_n\tilde{\mathbf{B}}_n^H]\}.\end{aligned} \tag{27}$$

Different from the conventional C-FBMC system, not all of the subcarriers are active in our C-FBMC-IM system. Compared with the conventional C-FBMC system where $k = L$, the MMSE equalization bias power of the C-FBMC-IM system is smaller since $k < L$ in equation (25). Besides, the processed noise power of the C-FBMC-IM system is the same with that of the conventional C-FBMC system according to (27). As a result, the error performance of the C-FBMC-IM system will be better than that of the C-FBMC system.

To detect the indices of the active subcarriers, the estimated symbol $\hat{\mathbf{s}}_n$ is divided into G groups by the detection group creator. Then, $\mathbf{T}_g$ can be detected by the optimal ML detector, which is expressed as

$$\hat{\mathbf{S}}_g = \arg\min_{\mathbf{S}_g\in\Lambda}\|\mathbf{T}_g - \mathbf{S}_g\|. \tag{28}$$

From $\hat{\mathbf{S}}_g$, we can decode the index bits by the index decoder and the constellation symbol bits by the symbol decoder. The complexity of ML detection is $\sim \mathcal{O}(2^{p_1}W^k)$.

To reduce the complexity of the ML detector, LLR detector is proposed in [2], whose complexity is $\sim \mathcal{O}(W)$. In C-FBMC-IM system, the LLR detector can be upgraded as

$$\begin{aligned}\lambda_m &= \ln(k) - \ln(L-k) \\ &\quad + \frac{|t_m|^2}{I_m} + \ln(\sum_{i=1}^{W}\exp(-\frac{1}{I_m}|t_m - w_i|^2)),\end{aligned} \tag{29}$$

where t_m represents the m-th subcarrier processed signal, I_m denotes the interference power of the m-th subcarrier and $w_i \in \mathcal{S}$ with $\mathcal{S}$ being the set of W-ary constellation symbols. After calculation of the L LLR values, the k subcarriers in each group are assumed to be active if they have maximum LLR values. In equation (29), the interference power can be calculated by

$$I_m = \mathrm{E}\|\mathbf{I}_{e,n}\|_m^2 + \mathrm{E}\|\mathbf{I}_{\eta,n}\|_m^2, \tag{30}$$

where $\mathrm{E}\|\mathbf{I}_{e,n}\|_m^2$ and $\mathrm{E}\|\mathbf{I}_{\eta,n}\|_m^2$ can be got by taking the m-th diagonal element of $\mathrm{E}\|\mathbf{I}_{e,n}\|^2$ and $\mathrm{E}\|\mathbf{I}_{\eta,n}\|^2$, respectively.

IV. Simulation results

In this section, simulations are carried out to validate the performance of the C-FBMC-IM system. The main parameters of the system are listed below:

- Sample rate: $F_s = 15.36Msps$
- Subcarrier frequency separation: $F_0 = 15KHz$
- Symbol duration: $T = 1/15000s$
- FFT/IFFT size: $M = 1024$
- Modulation mode: QPSK(W=4)

The 3GPP LTE standardized Extended Typical Urban (ETU) channel [20] is adopted in our simulations. The channel information is assumed to be known at the receiver. The Extended Gaussian Function (EGF) filter [21] is adopted in our simulation with overlapping factor $K = 4$ and $\alpha = 2$.

Fig. 3 shows the BER comparison of the C-FBMC-IM system and the C-FBMC system. For C-FBMC-IM sytem, (L, k) is set to $(4, 3)$ and $\rho = 1$, which means that the spectral efficiency of the C-FBMC-IM system is the same with that of the C-FBMC system. It can be found from the simulation result that the ML detector and the LLR detector exhibit exactly the same BER performance. By the utilization of subcarrier indices as a source of information, the C-FBMC-IM system outperforms the C-FBMC system. A performance gap of approximately 2dB is recorded for ZF equalizer and that is almost 3dB for MMSE equalizer. Since the MMSE equation bias power is reduced when we employ the IM technique, the C-FBMC-IM system with MMSE equalizer achieves a better BER performance than that with ZF equalizer.

In Fig. 4, (L, k) is set to $(8, 7)$ for the C-FBMC-IM system. The spectral efficiency of the C-FBMC-IM system is better

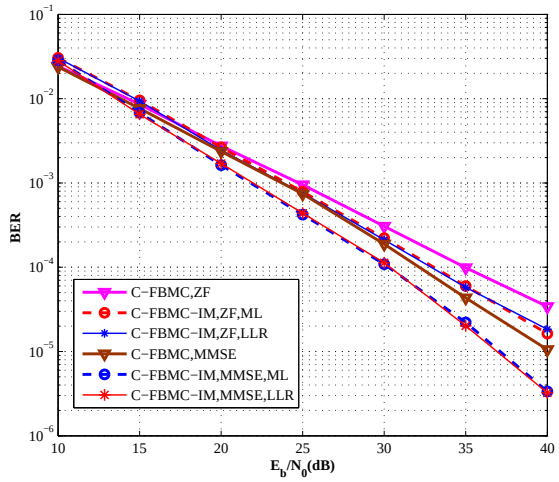

Fig. 3. The BER performance comparison of the C-FBMC-IM system and the C-FBMC system, with $\rho = 1$

than that of the C-FBMC system, with $\rho = 1.0625$. Almost the same BER performance can be achieved for the ML detector and the LLR detector. For ZF equalizer, the BER performance of the C-FBMC-IM system is 1dB worse than that of the C-FBMC system, which can be regarded as the expense paid for spectral efficiency improvement. However, for MMSE equalizer, because of the smaller MMSE equalization bias power, the BER performance of the C-FBMC-IM system can achieve 1dB better than that of the C-FBMC system. Both BER and spectral efficiency are improved when we introduce IM into the C-FBMC system.

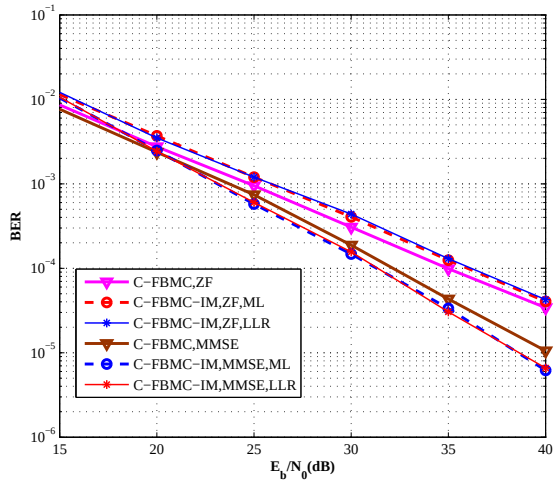

Fig. 4. The BER performance comparison of the C-FBMC-IM system and the C-FBMC system, with $\rho = 1.0625$

V. Conclusion

In this paper, we have introduced the IM technique in the C-FBMC system and build a C-FBMC-IM system model. In the multipath channel, the BER performance of the C-FBMC-IM system can be improved since the smaller MMSE equalization bias power. Furthermore, the ML detector and the LLR detector are upgraded for the C-FBMC-IM system. It has been demonstrated that the C-FBMC-IM system outperforms the C-FBMC system with the improvement of the spectral efficiency.

References

[1] R. Mesleh, H. Haas, S. Sinanovic, et al. "Spatial modulation," *IEEE Transactions on Vehicular Technology*, vol. 57, no. 4, pp. 2228-2241, July, 2008.

[2] E. Basar, U. Aygolu, E. Panayirci and H. V. Poor, "Orthogonal frequency division multiplexing with index modulation," *IEEE Transactions on Signal Processing*, vol. 61, no. 22, pp. 5536-5549, November, 2013.

[3] M. Wen, X. Cheng, M. Ma, B. Jiao and H. V. Poor, "On the achievable rate of OFDM with index modulation," *IEEE Transactions on Signal Processing*, vol. 64, no. 8, pp. 1919-1932, April, 2016.

[4] N. Ishikawa, S. Sugiura and L. Hanzo, "Subcarrier-Index Modulation Aided OFDM - Will It Work?," *IEEE Access*, vol. 4, pp. 2580-2593, May, 2016.

[5] B. Farhang-Boroujeny, "OFDM versus filter bank multicarrier," *IEEE Signal Processing Magazine*, vol. 28, no. 3, pp. 92-112, May, 2011.

[6] G. Fettweis, M. Krondorf, and S. Bittner, "GFDM - generalized frequency division multiplexing," *IEEE Vehicular Technology Conference*, pp. 1C4, April 2009.

[7] L. Zhang, A. Ijaz, P. Xiao, A. Quddus and R. Tafazolli, "Subband Filtered Multi-carrier Systems for Multi-service Wireless Communications," *IEEE Transactions on Wireless Communications*, vol. 16, no. 3, pp. 1893-1907, March, 2017.

[8] L. Zhang, A. Ijaz, P. Xiao, and R. Tafazolli, "Multi-service Systems: An Enabler of Flexible 5G Air-Interface," *IEEE Communications Magazine*, to appear, 2017.

[9] L. Zhang, P. Xiao, and A. Quddus, "Cyclic prefix-based universal filtered multicarrier system and performance analysis," *IEEE Signal Processing Letters*, vol. 23, no. 9, pp. 1197C1201, September, 2016.

[10] M. Bellanger, "Efficiency of filter bank multicarrier techniques in burst radio transmission," in *IEEE Global Telecommunications Conference (GLOBECOM)*, pp.1-4, December 2010.

[11] L. Zhang, A. Ijaz, P. Xiao, and R. Tafazolli, "Channel Equalization and Interference Analysis for Uplink Narrowband Internet of Things (NB-IoT)," *IEEE Communications Letters*, to appear, 2017. DOI: 10.1109/L-COMM.2017.2705710.

[12] A. Ijaz, L. Zhang, M. Grau, et al, "Enabling Massive IoT in 5G and Beyond Systems: PHY Radio Frame Design Considerations," *IEEE Access*, vol. 4, pp. 3322-3339, 2016.

[13] F. Wang, D. Qu, T. Jiang and B.Farhang-Boroujeny, "Tail shortening by virtual symbols in FBMC-OQAM signals," in *IEEE Signal Processing and Signal Processing Education Workshop (SP/SPE)*, pp.157-161, August, 2015.

[14] H. Lin and P. Siohan, "Multi-carrier modulation analysis and WCP-COQAM proposal," *EURASIP Journal on Advances in Signal Processing*, vol. 2014, no. 1, pp.1-19, 2014.

[15] Q. Duong and H. H. Nguyen, "Walsh-Hadamard precoded circular filterbank multicarrier communications," in *International Conference on Recent Advances in Signal Processing, Telecommunications and Computing (SigTelCom)*, pp. 193-198, January, 2017.

[16] S. Taheri, M. Ghoraishi, P. Xiao and L. Zhang, "Efficient implementation of filter bank multicarrier systems using circular fast convolution," *IEEE Access*, vol. 5, pp. 2855-2869, 2017.

[17] J. Zhang, M. Zhao, J. Zhong, P. Xiao and T. Yu, "Optimised index modulation for filter bank multicarrier system," *IET Communications*, vol. 11, no. 4, pp. 459-467, March, 2017.

[18] Y. Xiao, S. Wang, L. Dan, X. Lei, P. Yang and W. Xiang, "OFDM with interleaved subcarrier-index modulation," *IEEE Communications Letters*, vol. 18, no. 8, pp. 1447-1450, August, 2014.

[19] L. Zhang, P. Xiao, A. Zafar, A. U. Quddus and R.Tafazolli, "FBMC system: an insight into doubly dispersive channel impact," *IEEE Transactions on Vehicular Technology*, vol. 66, no. 5, pp. 3942-3956, May, 2017.

[20] E. Dahlman, S. Parkvall and J. Skold, "4G: LTE/LTE-advanced for mobile broadband," *Academic Press*, 2011.

[21] P. Siohan and C. Roche, "Cosine-modulated filterbanks based on extended Gaussian functions," *IEEE Transactions on Signal Processing*, vol. 48, no. 11, pp. 3052-3061, November, 2000.